Silymarin induces multiple myeloma cell apoptosis by inhibiting the JAK2/STAT3 signaling pathway

HAIYUN LIU[1], TINGTING LIU[2], JUNQUAN ZENG[3] and QUANGANG FANG[1]

[1]Department of Clinical Laboratory, Jiangxi Provincial People's Hospital, The First Affiliated Hospital of Nanchang Medical College, Nangchang, Jiangxi 330000, P.R. China; [2]Department of Hematology, Jiangxi Provincial People's Hospital, The First Affiliated Hospital of Nanchang Medical College, Nangchang, Jiangxi 330000, P.R. China; [3]Department of Hematology, The Affiliated Hospital of Jinggangshan University, Ji'an, Jiangxi 343000, P.R. China

Received December 18, 2024; Accepted May 22, 2025

DOI: 10.3892/ol.2025.15172

Abstract. Multiple myeloma (MM) is a malignant tumor that originates in the plasma cells of the bone marrow, interfering with the production of healthy blood cells and causing notable damage to bones and other tissues. Currently, the treatment options for MM are limited and often fail to provide effective and well-tolerated solutions. Silymarin, a primary active compound found in the dried fruit of *Silybum marianum*, is known for its inhibitory action on lipoxygenases and peroxidases. In addition to its known benefits in reducing liver toxicity and enhancing radiation protection, silymarin has shown promise in lowering lipid levels. Silymarin has anticancer properties; however, the specific mechanisms and efficacy of silymarin in treating MM require further investigation. In the present study, network pharmacology was employed to discern the targets and associated pathways of silymarin against MM. The cytotoxic effects of silymarin on MM were subsequently tested using RPMI 8226 and H929 cell lines. Furthermore, the molecular targets of silymarin in MM were assessed through immunofluorescence, reverse transcription-quantitative polymerase chain reaction and molecular docking studies. A total of 15 notable targets of silymarin associated with MM were identified, along with 60 interactions among these targets and several associated signaling pathways. *In vitro* experiments using Cell Counting Kit-8 and flow cytometry revealed that silymarin markedly promoted apoptosis in MM cells. Additionally, there was a reduction in the expression of anti-apoptotic genes, such as Bcl-2 and Bcl-xL. After silymarin treatment, a decrease in phosphorylation of JAK2 and STAT3 was observed in MM cells, and it was suggested that silymarin potentially binds to JAK2 and STAT3. In conclusion, silymarin was revealed to trigger apoptosis in MM cells by blocking the JAK2/STAT3 signaling pathway. This mechanism highlights the potential of silymarin as a therapeutic agent that can target specific molecular pathways to combat MM.

Correspondence to: Professor Quangang Fang, Department of Clinical Laboratory, Jiangxi Provincial People's Hospital, The First Affiliated Hospital of Nanchang Medical College, 92 Aiguo Road, Nangchang, Jiangxi 330000, P.R. China
E-mail: fqg173224668@163.com

Key words: network pharmacology, silymarin, JAK2/STAT3 signaling pathway, multiple myeloma, apoptosis, molecular docking

Introduction

Multiple myeloma (MM) is a malignant plasma cell disorder, originating from plasma cells in the bone marrow. As the final stage of B-lymphocyte development, MM is classified as a type of B-cell lymphoma (1). This disease is characterized by the abnormal proliferation of bone marrow plasma cells and the excessive production of monoclonal immunoglobulin light chain, with a minority of patients presenting with non-secreting MM (2). It is commonly associated with multiple lytic bone lesions, hypercalcemia, anemia and renal impairment (3,4). The suppression of normal immunoglobulin production in MM increases the risk of bacterial infections (5). The estimated incidence rate is 2-3 per 100,000, with a male-to-female ratio of 1.6:1, and most patients are >40 years old (6). Despite recent advancements in treatment, including proteasome inhibitors (such as bortezomib and carfilzomib), immunomodulatory drugs (such as lenalidomide and pomalidomide), monoclonal antibodies (such as daratumumab) and chimeric antigen receptor T-cell therapies, MM remains largely incurable due to drug resistance and cumulative toxicities (2,7). The median survival time for patients with relapsed/refractory MM is <12 months, highlighting the critical need for new treatments with improved safety and effectiveness (2,7).

Flavonoids, commonly found in plants, are classified as secondary metabolites, and include several medicinal compounds used in preventing and treating cardiovascular and cerebrovascular diseases (8). These compounds are known for their hepatoprotective, liver detoxification, antifungal, anti-inflammatory and antioxidant properties, which also boost immune function in animals (9). *Silybum marianum*, belonging to the Asteraceae family, produces silymarin in its fruit extract, which is known for its beneficial biological properties. Silymarin is widely used to treat conditions such as viral hepatitis, alcohol-related cirrhosis and liver cell damage (10,11). Silymarin, a bioactive component derived

from the seeds of milk thistle, is primarily recognized for inducing cellular apoptosis (12). *In vitro* studies have highlighted its potent anticancer effects, demonstrating the ability of this compound to inhibit a variety of cancer types, including both hormone-sensitive and hormone-insensitive types, such as skin, breast, bladder, lung and colon cancer (13,14). Additionally, silymarin has demonstrated antitumor activities in liver and prostate cancer by altering key cancer pathways, such as PI3K/AKT/mTOR and NF-κB signaling pathways, showcasing its extensive therapeutic potential (13,14). A previous study demonstrated that silymarin can inhibit the proliferation and induce apoptosis in the U266 MM cell line by modulating the PI3K/Akt/mTOR signaling pathway, thus indicating its potential as an anti-MM agent (15). However, due to the complex mechanisms of action and diverse targets of natural products, it is crucial to perform a comprehensive evaluation of the pharmacological effects of silymarin across various cell lines and to rigorously explore its mechanisms against MM.

The present study aimed to systematically evaluate the anti-myeloma effects of silymarin through an integrative approach combining network pharmacology, molecular docking and *in vitro* validation in RPMI 8226 and H929 cell lines. The study sought to identify key targets and signaling pathways underlying the activity of silymarin against MM, with a focus on apoptosis regulation and JAK2/STAT3 pathway modulation.

Materials and methods

Acquisition of target profiles of silymarin. To ensure highly reliable target spectrum data for silymarin, 10 target databases were accessed to gather both known and predicted target profiles, as shown in Table I. The UniProt database (http://www.uniprot.org) (16) was employed to standardize the names of the targets, and only genes corresponding to '*Homo sapiens*' were retained for further analysis.

MM gene collection. 'MM' was used as the search term to search for pathogenic genes associated with MM from five sources: Open Target Platform (17), DisGeNET (18), Comparative Toxicogenomics Database (19), GeneCards (20) and text mining. Gene names were standardized using DAVID v6.8 (https://david.abcc.ncifcrf.gov/) (21). To enhance data reliability, only genes that were confirmed or listed in ≥3 database sources were retained for further analysis.

Construction of silymarin target MM network. To identify potential candidate genes for silymarin in treating MM, the targets of silymarin were cross-referenced with genes associated with MM. The genes found at the intersection were regarded as prospective candidates for action of silymarin on MM. A network model was then created using Cytoscape software v3.7.1 (22) to depict the interactions between silymarin, its targets and MM.

To further identify the key targets of silymarin in treating MM, a protein-protein interaction (PPI) network was constructed through the online STRING database version 11.5 (https://string-db.org/) (23). The PPI networks were visualized using Cytoscape v3.7.1 (22). The central nodes in the network, or hub nodes, were assessed based on key topological parameters, specifically the degree (24). The NetworkAnalyzer plugin (25) was employed to calculate the degree (24).

Table I. Target database information for identifying silymarin targets.

Target source	Target type	(Refs.)
TargetNet	Putative target	(48)
SwissTargetPrediction	Putative target	(49)
ChEMBL prediction	Putative target	(50)
BATMAN-TCM	Putative target	(51)
STITCH	Putative target	(52)
DrugBank	Known target	(53)
TTD	Known target	(54)
ChEMBL	Known target	(55)
PubChem	Known target	(28)
CTD	Known target	(56)

CTD, Comparative Toxicogenomics Database; STITCH, search tool for interactions of chemicals; TTD, Therapeutic Target Database.

Gene ontology (GO) and kyoto encyclopedia of genes and genomes (KEGG) enrichment analyses. GO and KEGG enrichment analyses for the candidate genes of silymarin in MM were performed using clusterProfiler version 4.0.3, an R Bioconductor package (26). During enrichment analysis, the thresholds for the P-value and q-value were set at 0.05. This criterion was used to determine the significantly enriched GO terms and KEGG pathways associated with the candidate genes.

Molecular docking. The molecular docking method was employed to virtually assess the binding affinity between the compound and target proteins, providing a basis for subsequent experimental validation. AutoDock Vina 1.1.2, an open-source software for molecular docking and virtual screening, offers markedly improved accuracy in predicting binding modes compared with AutoDock 4 (27). A spatial data file format of silymarin was downloaded from the PubChem database (https://pubchem.ncbi.nlm.nih.gov/) (28) and converted into Mol2 format using Open Babel 2.4.1 (29). The crystal structure of JAK2 [Protein Data Bank (PDB) identification (ID), 3UGC] and STAT3 (PDB ID, 6NJS) were downloaded from the PDB database (https://www.rcsb.org/) (30) NVP-BBT594 (PubChem CID, 59596344) and SD36 (PubChem CID, 139600321), co-crystalline ligands of JAK2 and STAT3 respectively, were selected as positive controls. Small molecules were energy minimized using PyRx-0.8 software (Dr. Sargis Dallakyan; The Scripps Research Institute). Both ligands and receptors were prepared following the AutoDock Vina 1.1.2 tutorial. During rigid docking, grid properties were determined based on the spatial position of the co-crystallized ligands within the proteins. Each structure was prepared by removing water molecules, adding non-polar hydrogen, calculating Gasteiger charges and saving in PDBQT format. Typically, a lower Vina score indicates a higher affinity between the ligand and receptor, with a general threshold for

Table II. Primer information.

Gene	Forward primer (5'-3')	Reverse primer (5'-3')
Human Bcl-2 (NM_000633)	ATCGCCCTGTGGATGACTGAGT	GCCAGGAGAAATCAAACAGAGGC
Human Bcl-xL (NM_138578)	GCCACTTACCTGAATGACCACC	AACCAGCGGTTGAAGCGTTCCT
Human GAPDH (NM_002046)	GTCTCCTCTGACTTCAACAGCG	ACCACCCTGTTGCTGTAGCCAA

binding energy being ≤-5 kcal/mol (31,32). The interaction modes between the compound and target proteins were visualized using PyMOL software version 3.1 (Schrödinger, Inc.).

Cell culture. The RPMI 8226 and H929 cell lines were obtained from American Type Culture Collection. These cell lines were cultured in RPMI 1640 medium (Gibco; Thermo Fisher Scientific, Inc.), supplemented with 10% fetal bovine serum (Biological Industries), and maintained without antibiotics at 37˚C in an incubator with 5% CO_2. The culture medium was refreshed every 2 days.

Cell viability assay. A total of $1x10^5$ cells/well were seeded in 96-well plates. The cells were treated with silymarin (cat. no. HY-N7073; MedChemExpress) dissolved in dimethyl sulfoxide (DMSO) at gradient concentrations from 0 to 100 μM (in 10 μM increments), or with vehicle control (0.1% DMSO, equivalent to the highest solvent concentration in treatment groups) for 24 h at 37˚C prior to the addition of Cell Counting Kit-8 (CCK-8) reagent. A total of 100 ml serum-free medium supplemented with 10 ml CCK-8 reagent (MilliporeSigma) was then added to each well and incubated for 2 h at 37˚C in the dark. Cell viability was assessed by measuring the absorbance at 450 nm using a spectrophotometric plate reader (BioTek; Agilent Technologies, Inc.).

Flow cytometry. In a preliminary experiment, cells began to die within 24 h of silymarin administration when examined under a microscope. Therefore, 24 h was selected as the treatment duration. After the treatment of RPMI 8226 or H929 cells, which were seeded into 6-well plates at a density of $1x10^6$ cells/well, with 50 μM silymarin for 24 h at 37˚C, the cells were collected and centrifuged at 1,000 x g for 5 min at 4˚C. The cell suspensions were then washed twice with chilled phosphate-buffered saline (PBS) and incubated with 10 μl Annexin-V FITC (100 mg/ml; BD Biosciences) for 30 min in the dark. Subsequently, 5 μl PI (100 mg/ml; BD Biosciences) was added, and the cells were incubated for an additional 30 min in the dark on ice. Apoptotic rates were analyzed using flow cytometry (FACSCalibur; BD Biosciences). Data acquisition was performed with BD CellQuest™ Pro software (version 5.2; BD Biosciences), and quantitative analysis was conducted using FlowJo software (version 10.8.1; FlowJo LLC).

RNA isolation and reverse transcription-quantitative PCR (RT-qPCR). Total RNA from RPMI 8226 and H929 cells was isolated using the TransZol Up Plus RNA Kit (cat. no. ER501-01; TransGen Biotech Co., Ltd.) and subsequently reverse transcribed using the GoScript™ Reverse Transcription System (cat. no. A5001; Promega Corporation). The resulting cDNA was used as a template for qPCR, which was performed using the MonAmp™ ChemoHS qPCR Mix kit (cat. no. MQ00401S; Monad Biotech Co., Ltd.). The primer sequences used are detailed in Table II. The following thermocycling protocol was used: Stage 1, activation at 50˚C for 2 min; stage 2, pre-soak at 95˚C for 10 min; stage 3, 40 cycles of denaturation at 95˚C for 15 sec, annealing at 60˚C for 1 min; stage 4, melting curve, 95˚C for 15 sec, 60˚C for 15 sec, 95˚C for 15 sec. All procedures were performed according to the manufacturer's guidelines.

Immunofluorescence. Cells were fixed with 4% paraformaldehyde for 10 min at room temperature, followed by permeabilization with 0.1% Triton X-100 for 15 min. Subsequently, 5% bovine serum albumin (BSA; cat. no. A9418; MilliporeSigma) was applied to block nonspecific binding for 15 min. Primary antibodies targeting JAK2 (1:500; cat. no. PA5-11267; Thermo Fisher Scientific, Inc.), phosphorylated-JAK2 (1:500; cat. no. PA5-99341; Thermo Fisher Scientific, Inc.), STAT3 (1:100; cat. no. MA1-13042; Thermo Fisher Scientific, Inc.) and phosphorylated-STAT3 (1:100; cat. no. PA5-17876; Thermo Fisher Scientific, Inc.) were added to the cells and incubated overnight at 4˚C. After washing three times with PBS, the cells were incubated with Alexa Fluor™ 488-conjugated goat anti-rabbit IgG (1:500; cat. no. SA00013-2; Proteintech Group, Inc.) for JAK2, p-JAK2, and p-STAT3 detection, and Alexa Fluor™ 594-conjugated goat anti-mouse IgG (1:500; cat. no. SA00013-3; Proteintech Group, Inc.) for STAT3 at 37˚C for 1 h. Nuclei were stained with DAPI (1 μg/ml) for 15 min in the dark prior to imaging. Imaging was performed using a ZEISS laser scanning confocal microscope (ZENA GmbH). Quantitative analysis of fluorescence intensity was conducted using ImageJ software (version 1.53q; National Institutes of Health) by defining regions of interest (ROIs) around nuclei (DAPI channel) and measuring mean pixel intensity in corresponding JAK2/STAT3 channels. Data were normalized to background fluorescence (unstained controls) and expressed as fold change relative to control groups.

Statistical analysis. All results are presented as the mean ± standard deviation for normally distributed data or median (interquartile range) for non-normally distributed data. Statistical analyses were performed using SPSS 22 (IBM Corp.). Initially, data were tested for normal distribution using the Shapiro-Wilk test and for homogeneity of variances using Levene's test. Based on these results, appropriate statistical tests were selected. One-way analysis of variance (ANOVA) was utilized to assess the significance of differences in normally distributed data, followed by

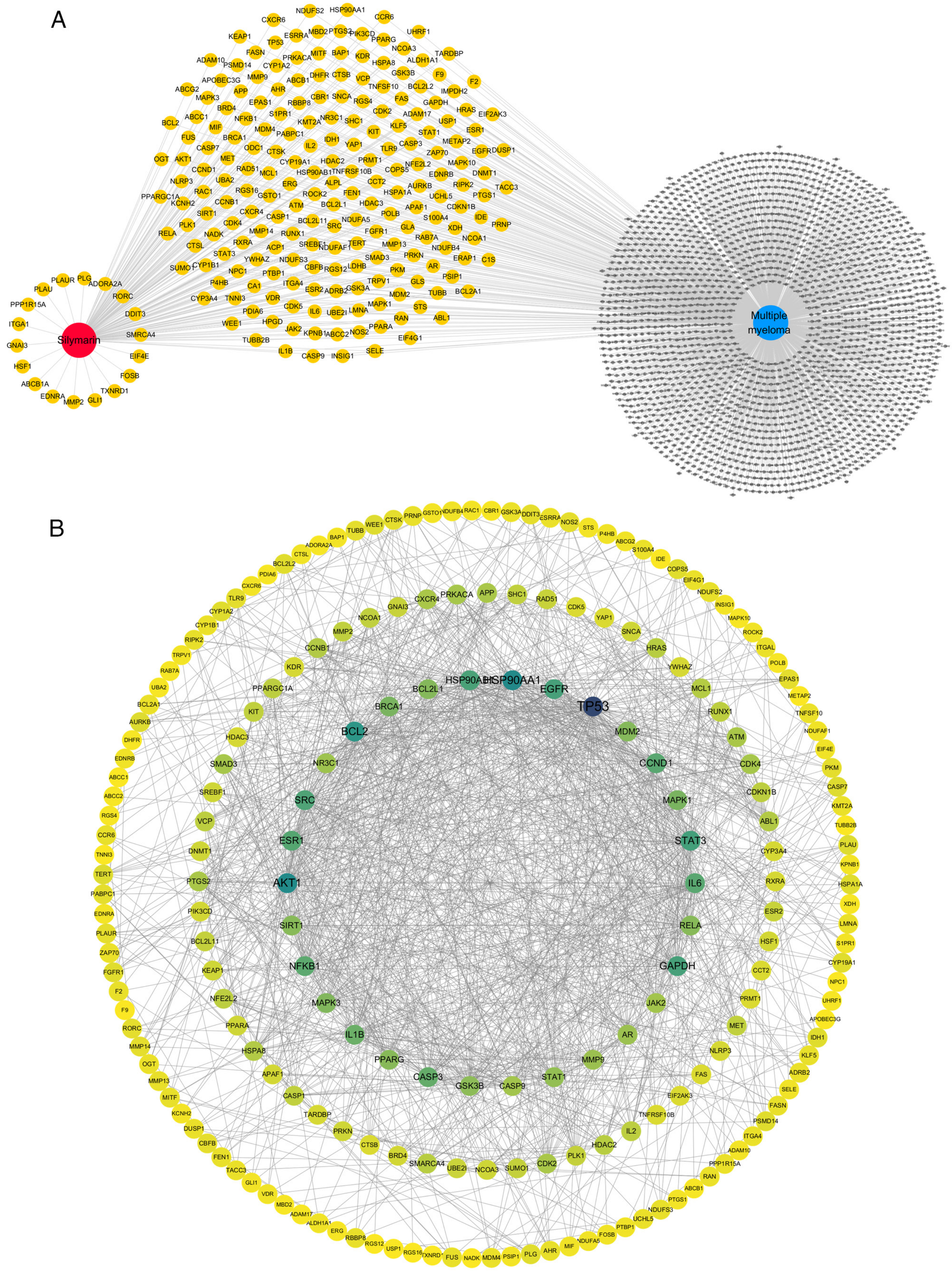

Figure 1. Analysis of overlapping targets between silymarin and MM. (A) Overlap of gene targets associated with both MM and silymarin. The red node represents silymarin, the blue node represents MM, the yellow nodes represent silymarin targets and the gray nodes represent MM genes. (B) Protein-protein interaction network of the shared targets. The color depth of nodes is directly proportional to the degree of nodes. The darker the color, the greater the degree of nodes and the lighter the color, the smaller the degree of nodes. MM, multiple myeloma.

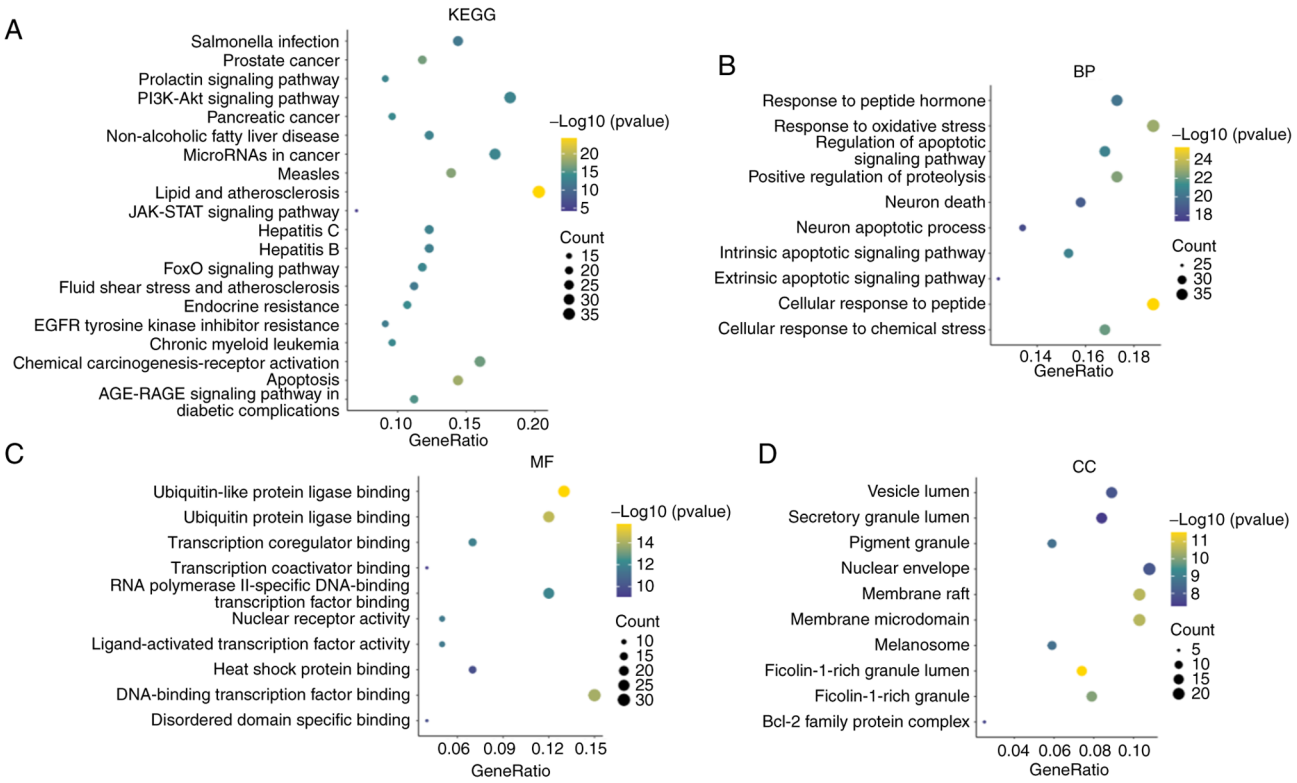

Figure 2. Enrichment analysis of potential targets of silymarin in multiple myeloma treatment. (A) KEGG enrichment analysis. Analyses of enriched (B) BP, (C) MF and (D) CC. The color of the dots is associated with the P-value. The size of the dots represents the number of genes, and the larger the dots the more genes there are. KEGG, Kyoto Encyclopedia of Genes and Genomes; BP, biological processes; MF, molecular functions; CC, cellular components.

Dunnett's multiple comparisons test. For data that were not normally distributed, the Kruskal-Wallis test was applied followed by Dunn's test. For comparisons between two independent groups, an independent Student's t-test was applied. $P<0.05$ was considered to indicate a statistically significant difference for all analyses.

Results

Construction of target network between silymarin and MM. From 10 target databases, a comprehensive set of 594 targets associated with silymarin, encompassing both known and predicted targets, was compiled. Additionally, by querying six databases and selecting only those genes appearing in at ≥3 sources, a total of 2,178 genes strongly associated with MM were identified. Intersection analysis of the silymarin targets and MM genes revealed 221 common genes. These genes were considered potential targets for silymarin in the treatment of MM and were selected for further analysis (Fig. 1A).

The 221 overlapping targets identified were subsequently uploaded into the STRING database to construct a PPI network. The resulting PPI network data were exported as a TSV file and subsequently analyzed using Cytoscape, revealing 209 connected targets and 1,359 interactions between them. Analysis of the network based on degree centrality highlighted several key targets including TP53, HSP90AA1, AKT1, BCL2, STAT3, GAPDH, EGFR, HSP90AB1, SRC, ESR1, IL6, CCND1, NFKB1, CASP3, IL1B, BRCA1, MAPK1, MAPK3, BCL2L1, MDM2, RELA, PPARG, SIRT1, GSK3B, STAT1, AR, MMP9, NR3C1, JAK2 and CASP9 (Fig. 1B).

GO and KEGG enrichment analyses of candidate genes of silymarin in MM. The candidate genes of silymarin in MM were enriched in 159 pathways, including 'Apoptosis', 'Prostate cancer', 'Chemical carcinogenesis-receptor activation', 'JAK-STAT signaling pathway', 'Endocrine resistance', 'Pancreatic cancer', 'Chronic myeloid leukemia', 'FoxO signaling pathway', 'MicroRNAs in cancer', 'Prolactin signaling pathway' and 'PI3K-Akt signaling pathway' (Fig. 2A). Silymarin was also suggested to exert therapeutic effects on MM by engaging in 2,287 biological processes, such as 'cellular response to peptide', 'response to oxidative stress', 'positive regulation of proteolysis', 'cellular response to chemical stress' and 'regulation of apoptotic signaling pathway' (Fig. 2B). Additionally, silymarin in MM was noted to be involved in 191 molecular functions, including 'ubiquitin-like protein ligase binding', 'ubiquitin protein ligase binding', 'DNA-binding transcription factor binding', 'RNA polymerase II-specific DNA-binding transcription factor binding' and 'transcription coregulator binding' (Fig. 2C). Furthermore, it was demonstrated to interact with 89 cellular components, including 'membrane raft', 'membrane microdomain', 'protein kinase complex', 'transferase complex' and 'serine/threonine protein kinase complex' (Fig. 2D).

Silymarin induces the apoptosis of MM cells. To evaluate the therapeutic effects of silymarin on MM, its impact on cell viability was investigated using the CCK-8 assay. The dose-response curves demonstrated that silymarin has a dose-dependent inhibitory effect on cell viability in both MM cell lines (Fig. 3A and B). Furthermore, flow cytometric

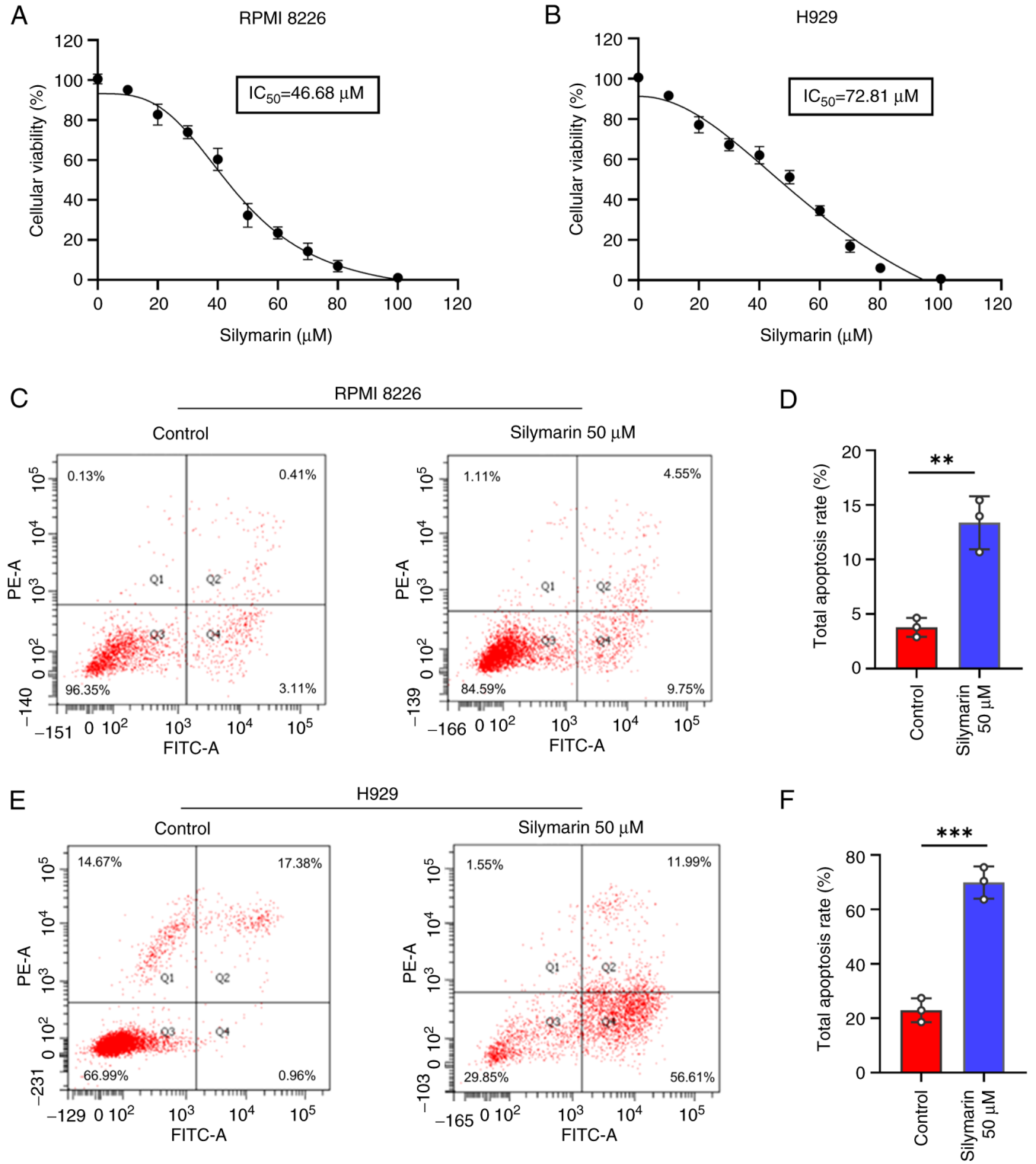

Figure 3. Silymarin induces the apoptosis of MM cells *in vitro*. Dose-response curves of silymarin on MM cell lines, (A) RPMI 8226 and (B) H929, as determined by a Cell Counting Kit-8 assay. (C and D) Silymarin promoted the apoptosis of RPMI 8226 cells. (E and F) Silymarin promoted the apoptosis of H929 cells. n=3; **P<0.01; ***P<0.001. Error bars indicate standard deviation. MM, multiple myeloma.

analysis revealed that silymarin promoted early and late apoptosis in MM cells compared with that in the control groups (Fig. 3C-F).

Silymarin inhibits the JAK2/STAT3 signaling pathway in MM cell lines. Network pharmacology analysis identified JAK2 and STAT3 as central nodes within the PPI network (Fig. 1B), and KEGG enrichment analysis pinpointed the 'JAK-STAT signaling pathway' as a crucial mechanism of silymarin in MM (Fig. 2A). Previous research has reported that inhibiting the JAK2/STAT3 pathway can induce apoptosis in MM cells (30,31). These results suggested that the JAK2/STAT3

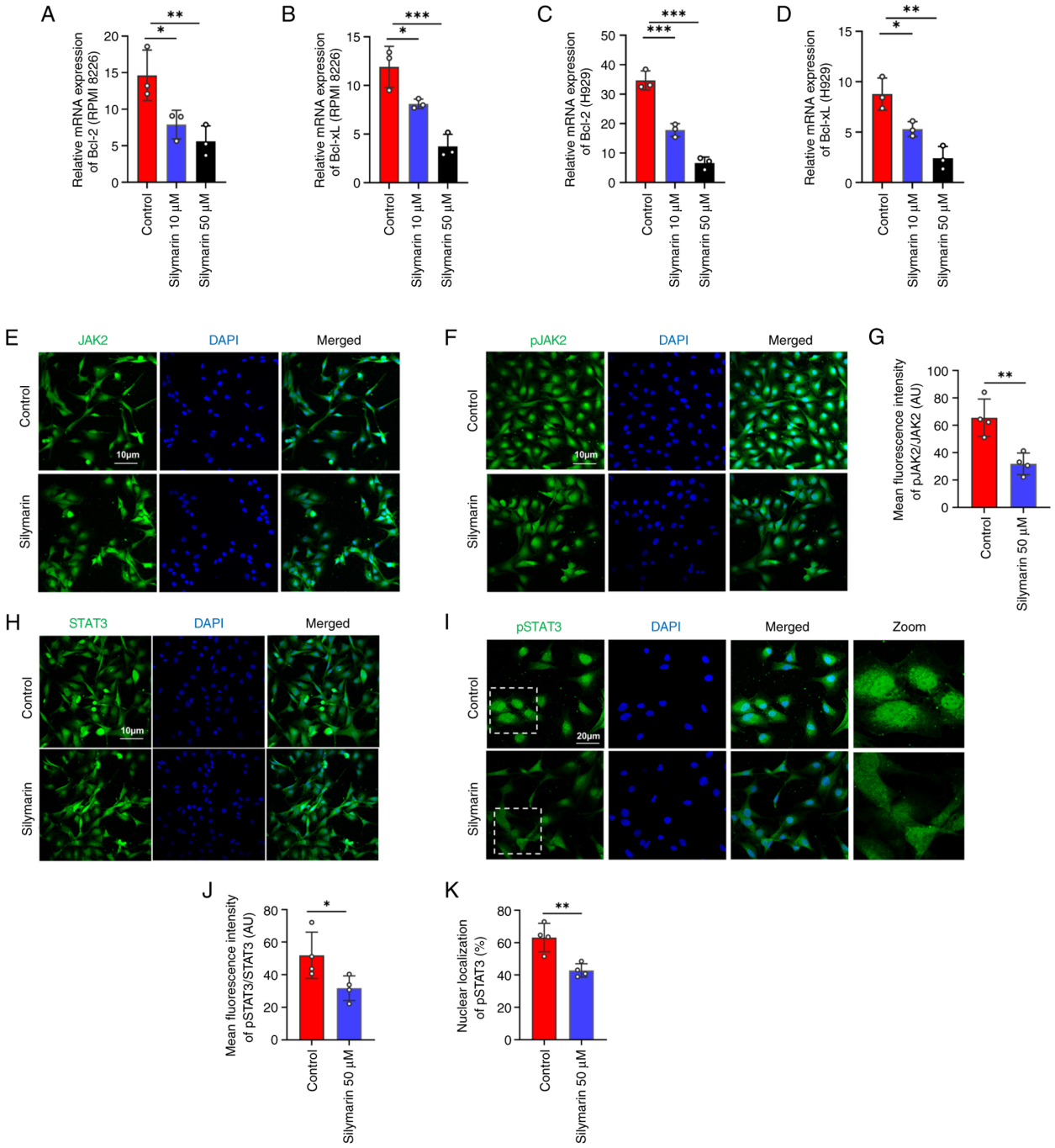

Figure 4. Silymarin inhibits the JAK2/STAT3 signaling pathway in multiple myeloma cells. mRNA expression levels of (A) Bcl-2 and (B) Bcl-xL in the RPMI 8226 cell line (n=3). mRNA expression levels of (C) Bcl-2 and (D) Bcl-xL in the H929 cell line (n=3). Immunofluorescence images of (E) JAK2 and (F) pJAK2. (G) Semi-quantification of levels of pJAK2 in the RPMI 8226 cell line (n=4). Immunofluorescence images of (H) STAT3 and (I) pSTAT3. Semi-quantification of (J) levels of pSTAT3 and (K) nuclear localization of pSTAT3 in the RPMI 8226 cell line (n=4). *P<0.05; **P<0.01; ***P<0.001. Error bars indicate standard deviation. p, phosphorylated; AU, arbitrary units.

pathway may be notable in apoptosis induced by silymarin. To further evaluate the molecular mechanisms by which silymarin can induce MM apoptosis, the expression of the anti-apoptotic genes Bcl-2 and Bcl-xL, which are transcriptional targets of JAK2/STAT3 signaling, were assessed in silymarin-treated MM cells. The results demonstrated that silymarin reduced the expression levels of Bcl-2 and Bcl-xL in the tested MM cell lines at both 10 and 50 μM compared with those in the control groups (Fig. 4A-D). Moreover, the phosphorylation and nuclear localization of JAK2 and STAT3 were reduced with silymarin treatment compared with those in the control groups (Fig. 4E-K). Collectively, these findings indicated that silymarin may inhibit the JAK2/STAT3 signaling pathway.

Validation of molecular docking between silymarin, JAK2 and STAT3. At the molecular level, silymarin was demonstrated to potentially interact with JAK2 and STAT3. Based on empirical rules, the effective binding energy between small molecules and target protein should be <-5 kcal/mol. The present findings of molecular docking analysis indicated that silymarin has a

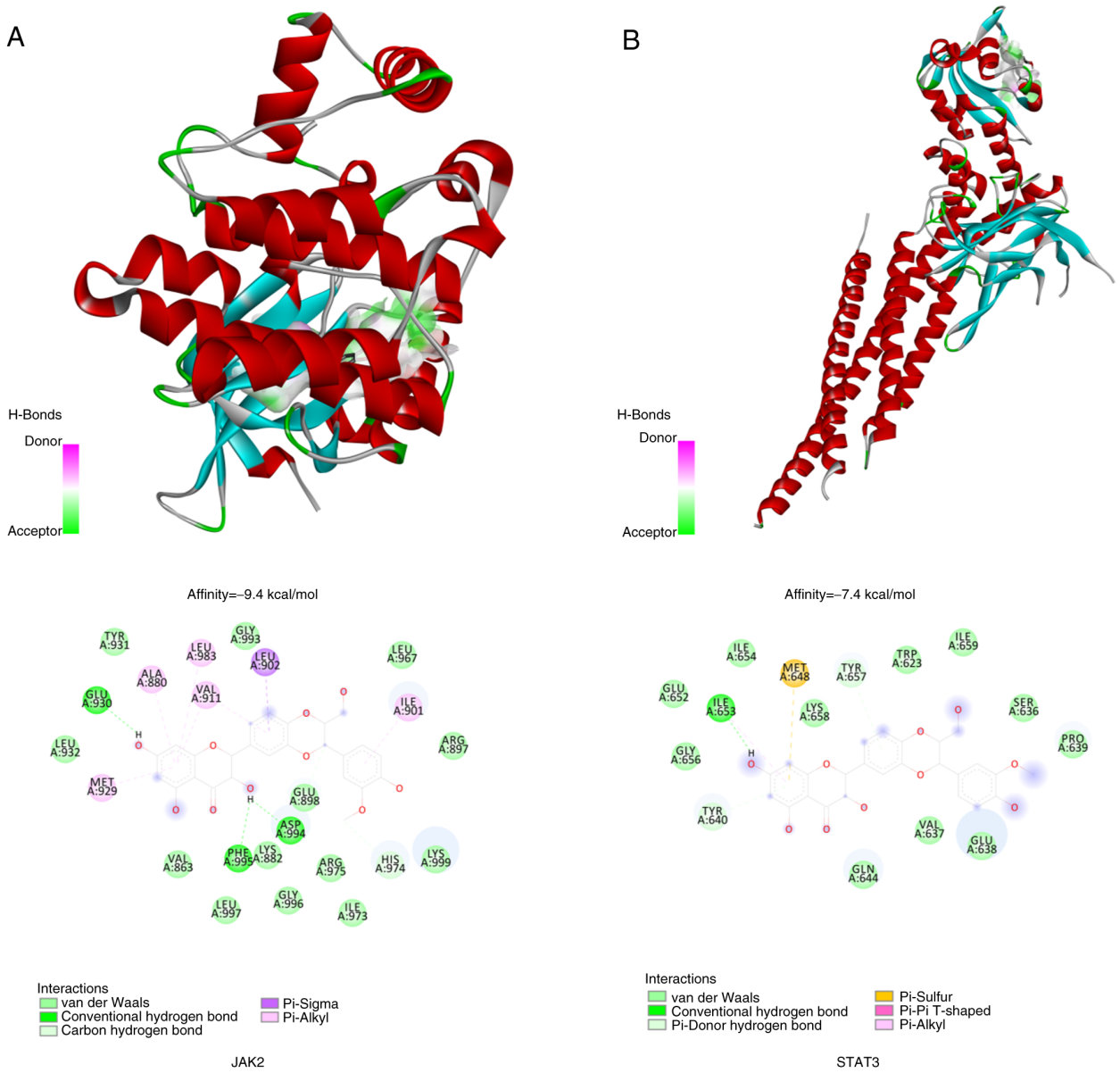

Figure 5. Interaction mode between silymarin and JAK2/STAT3. (A) Docking diagram of silymarin and JAK2 protein. (B) Docking diagram of silymarin and STAT3 protein. In addition, the planar structure of silymarin can be seen in the 2D image.

particularly high affinity for JAK2, with a binding energy of -9.4 kcal/mol (Fig. 5A). The docking analysis of silymarin with JAK2 suggested that silymarin fits well into the active site of the JAK2 protein. It was shown to form hydrogen bonds with the amino acids Glu930, Asp994 and Phe995 and to engage in a pi-sigma interaction with Leu902. Additionally, pi-alkyl interactions were noted with Leu901, Leu983, Val911, Ala880 and Met929. In the silymarin-STAT3 protein docking model (Fig. 5B), silymarin was shown to be located within the binding site of the STAT3 protein, where it can form hydrogen bonds with Ile653 and pi-sulfur interactions with Met648, along with pi-alkyl interactions with Ile653.

Discussion

Network pharmacology has become an invaluable tool for research and development in the field of natural products. In previous years, notable advancements have been made in developing network pharmacology methods and applying them to uncover the scientific basis of natural medicines. This includes identifying new targets, discovering potential bioactive compounds and elucidating mechanisms of action (33). Thus, by integrating network pharmacology with experimental validation, researchers can enhance their understanding of how natural compounds function and drive innovation in natural product development. The present study demonstrated the therapeutic potential of silymarin in treating MM through both computational and laboratory experiments. Specifically, the results indicated that silymarin can target the JAK2/STAT3 signaling pathway, interacting with JAK2 and STAT3 proteins to promote cytotoxicity and apoptosis in MM cells. The effectiveness of silymarin was evaluated in two MM cell lines.

The enrichment analysis of silymarin treatment in MM revealed significant modulation of 159 pathways, highlighting its multifaceted therapeutic potential. Key pathways influenced

by silymarin includes the 'JAK-STAT signaling pathway', 'PI3K-Akt signaling pathway' and 'FoxO signaling pathway', all of which are involved in cancer cell survival, proliferation and apoptosis (34-36). The 'JAK-STAT signaling pathway', known for its role in cytokine signaling and cancer progression, was notably affected, suggesting that silymarin may disrupt the survival signals in MM cells, thereby promoting apoptosis. This is consistent with previous studies demonstrating the anti-cancer properties of silymarin through the inhibition of STAT3 activation in various cancer models (37,38). Additionally, the 'PI3K-Akt signaling pathway', a central regulator of cell proliferation and metabolism, was modulated by silymarin. This pathway is frequently dysregulated in MM, contributing to drug resistance and disease progression. The ability of silymarin to inhibit this pathway may enhance the sensitivity of MM cells to conventional therapies, as evidenced by its role in reversing endocrine resistance in other types of cancer, such as breast cancer (39). Furthermore, the 'FoxO signaling pathway', which is involved in cellular stress responses and apoptosis, was impacted, suggesting that silymarin may activate FoxO-mediated apoptotic mechanisms in MM cells.

The enrichment analysis also highlighted the influence of silymarin on specific cancer pathways, such as 'Prostate cancer', 'Pancreatic cancer' and 'Chronic myeloid leukemia'. This broad-spectrum activity underscores the potential of silymarin as a multi-targeted therapeutic agent. Notably, the modulation of the 'MicroRNAs in cancer' pathway further supported its role in epigenetic regulation, which could be pivotal in overcoming drug resistance in MM, for example, by upregulating tumor-suppressive miR-223-3p and miR-16-5p, and downregulating miR-92-3p, thereby suppressing pro-survival signals (40).

The JAK family of intracellular non-receptor tyrosine kinases is known to transmit signals via the JAK/STAT pathway, triggered by cytokines as described previously (41,42). The JAK/STAT signaling pathway involves a sequence of interactions between intracellular proteins, which are crucial for immune responses, cell proliferation, apoptosis and cancer development (41,42). Previous research has demonstrated that the transcription factor STAT3 is constitutively active in the majority of patients with MM (43). Typically, STAT3 is rapidly and transiently activated by cytokines; however, persistent STAT3 activation in myeloma cells leads to increased expression of genes associated with cell proliferation, metastasis and resistance to treatment, such as CCND1, MMP9 and BIRC5 (44). The constitutive activation of STAT3 can occur through several mechanisms, including autocrine or paracrine loops, notably with IL6, or the lack of negative regulators (45). A previous study indicated that silymarin possesses STAT inhibitory properties, leading to the activation of caspases and apoptosis in human prostate cancer cells (46). In MM, the JAK/STAT signaling pathway is a vital target for silymarin, with potential as a biomarker for its therapeutic application in treating this disease. Additionally, the present results revealed the ability of silymarin to bind to JAK2 and potentially modulate the JAK/STAT pathway by inhibiting JAK2 activity.

In conclusion, the findings suggested that silymarin exerts its anti-MM effects through the modulation of key signaling pathways involved in apoptosis and cell proliferation. These results provide a strong rationale for further preclinical and clinical investigations into silymarin as a promising therapeutic agent for MM. Future studies should focus on validating these pathways using *in vivo* models and exploring potential synergies with existing MM therapies. Silymarin, a commonly used component in traditional Chinese medicine, is known for its minimal side effects according to a previous study (47). The limitations of the experimental conditions prevented direct detection of caspase activation, thereby compromising the objectivity of the conclusions and representing a key limitation of the present study. Although caspase activation was not directly measured, the observed downregulation of anti-apoptotic proteins Bcl-2/Bcl-xL and the induction of apoptosis, measured by flow cytometry, collectively suggested the involvement of caspase-mediated pathways in apoptosis. As a result, silymarin may be considered a promising option for expanding the range of treatments available for MM, potentially enhancing patient outcomes with its safe profile and effective therapeutic action.

Acknowledgements

Not applicable.

Funding

The present study was sponsored by the Jiangxi Provincial Health Technology Project (grant no. 202410118).

Availability of data and materials

The data generated in the present study may be requested from the corresponding author.

Authors' contributions

Conceptualization was performed by TL and HL. The methodology, experiments and statistical analysis were performed by HL, QF and JZ. The manuscript was written by JZ and HL. HL performed the project administration. All authors read and approved the final version of the manuscript. TL and HL confirm the authenticity of all the raw data.

Ethics approval and consent to participate

Not applicable.

Patient consent for publication

Not applicable.

Competing interests

The author declare that they have no competing interests.

References

1. Raab MS, Podar K, Breitkreutz I, Richardson PG and Anderson KC: Multiple myeloma. Lancet 374: 324-339, 2009.
2. Cowan AJ, Green DJ, Kwok M, Lee S, Coffey DG, Holmberg LA, Tuazon S, Gopal AK and Libby EN: Diagnosis and management of multiple myeloma: A review. JAMA 327: 464-477, 2022.

3. Choi T, Ahn W, Shin DW, Han K, Kim D and Chun S: Association between kidney function, proteinuria and the risk of multiple myeloma: A population-based retrospective cohort study in South Korea. Cancer Res Treat 54: 926-936, 2022.
4. Korbet SM and Schwartz MM: Multiple myeloma. J Am Soc Nephrol 17: 2533-2545, 2006.
5. Rajkumar SV: Myeloma today: Disease definitions and treatment advances. Am J Hematol 91: 90-100, 2016.
6. Turesson I, Bjorkholm M, Blimark CH, Kristinsson S, Velez R and Landgren O: Rapidly changing myeloma epidemiology in the general population: Increased incidence, older patients, and longer survival. Eur J Haematol: April 9, 2018 (Epub ahead of print).
7. Malard F, Neri P, Bahlis NJ, Terpos E, Moukalled N, Hungria VTM, Manier S and Mohty M: Multiple myeloma. Nat Rev Dis Primers 10: 45, 2024.
8. Deng Y, Tu Y, Lao S, Wu M, Yin H, Wang L and Liao W: The role and mechanism of citrus flavonoids in cardiovascular diseases prevention and treatment. Crit Rev Food Sci Nutr 62: 7591-7614, 2022.
9. Majee C, Mazumder R, Choudhary AN and Salahuddin: An insight into the hepatoprotective activity and structure-activity relationships of flavonoids. Mini Rev Med Chem 23: 131-149, 2023.
10. Mohammadi S, Ashtary-Larky D, Asbaghi O, Farrokhi V, Jadidi Y, Mofidi F, Mohammadian M and Afrisham R: Effects of silymarin supplementation on liver and kidney functions: A systematic review and dose-response meta-analysis. Phytother Res 38: 2572-2593, 2024.
11. Gillessen A and Schmidt HH: Silymarin as supportive treatment in liver diseases: A narrative review. Adv Ther 37: 1279-1301, 2020.
12. Wadhwa K, Pahwa R, Kumar M, Kumar S, Sharma PC, Singh G, Verma R, Mittal V, Singh I, Kaushik D and Jeandet P: Mechanistic insights into the pharmacological significance of silymarin. Molecules 27: 5327, 2022.
13. Delmas D, Xiao J, Vejux A and Aires V: Silymarin and cancer: A dual strategy in both in chemoprevention and chemosensitivity. Molecules 25: 2009, 2020.
14. Koltai T and Fliegel L: Role of silymarin in cancer treatment: Facts, hypotheses, and questions. J Evid Based Integr Med 27: 2515690X211068826, 2022.
15. Feng N, Luo J and Guo X: Silybin suppresses cell proliferation and induces apoptosis of multiple myeloma cells via the PI3K/Akt/mTOR signaling pathway. Mol Med Rep 13: 3243-3248, 2016.
16. UniProt Consortium: UniProt: The universal protein knowledgebase in 2025. Nucleic Acids Res 53 (D1): D609-D617, 2025.
17. Carvalho-Silva D, Pierleoni A, Pignatelli M, Ong C, Fumis L, Karamanis N, Carmona M, Faulconbridge A, Hercules A, McAuley E, *et al*: Open targets platform: New developments and updates two years on. Nucleic Acids Res 47 (D1): D1056-D1065, 2019.
18. Piñero J, Saüch J, Sanz F and Furlong LI: The DisGeNET cytoscape app: Exploring and visualizing disease genomics data. Comput Struct Biotechnol J 19: 2960-2967, 2021.
19. Davis AP, Grondin CJ, Johnson RJ, Sciaky D, McMorran R, Wiegers J, Wiegers TC and Mattingly CJ: The comparative toxicogenomics database: Update 2019. Nucleic Acids Res 47 (D1): D948-D954, 2019.
20. Safran M, Dalah I, Alexander J, Rosen N, Iny Stein T, Shmoish M, Nativ N, Bahir I, Doniger T, Krug H, *et al*: GeneCards version 3: The human gene integrator. Database (Oxford) 2010: baq020, 2010.
21. Dennis G Jr, Sherman BT, Hosack DA, Yang J, Gao W, Lane HC and Lempicki RA: DAVID: Database for annotation, visualization, and integrated discovery. Genome Biol 4: P3, 2003.
22. Shannon P, Markiel A, Ozier O, Baliga NS, Wang JT, Ramage D, Amin N, Schwikowski B and Ideker T: Cytoscape: A software environment for integrated models of biomolecular interaction networks. Genome Res 13: 2498-2504, 2003.
23. Szklarczyk D, Morris JH, Cook H, Kuhn M, Wyder S, Simonovic M, Santos A, Doncheva NT, Roth A, Bork P, *et al*: The STRING database in 2017: Quality-controlled protein-protein association networks, made broadly accessible. Nucleic Acids Res 45 (D1): D362-D368, 2017.
24. Karbalaei R, Allahyari M, Rezaei-Tavirani M, Asadzadeh-Aghdaei H and Zali MR: Protein-protein interaction analysis of Alzheimer's disease and NAFLD based on systems biology methods unhide common ancestor pathways. Gastroenterol Hepatol Bed Bench 11: 27-33, 2018.
25. Assenov Y, Ramírez F, Schelhorn SE, Lengauer T and Albrecht M: Computing topological parameters of biological networks. Bioinformatics 24: 282-284, 2008.
26. Yu G, Wang LG, Han Y and He QY: clusterProfiler: An R package for comparing biological themes among gene clusters. OMICS 16: 284-287, 2012.
27. Trott O and Olson AJ: AutoDock Vina: Improving the speed and accuracy of docking with a new scoring function, efficient optimization, and multithreading. J Comput Chem 31: 455-461, 2010.
28. Kim S, Thiessen PA, Bolton EE, Chen J, Fu G, Gindulyte A, Han L, He J, He S, Shoemaker BA, *et al*: PubChem substance and compound databases. Nucleic Acids Res 44 (D1): D1202-D1213, 2016.
29. O'Boyle NM, Banck M, James CA, Morley C, Vandermeersch T and Hutchison GR: Open Babel: An open chemical toolbox. J Cheminform 3: 33, 2011.
30. Karuppasamy MP, Venkateswaran S and Subbiah P: PDB-2-PBv3.0: An updated protein block database. J Bioinform Comput Biol 18: 2050009, 2020.
31. Li B, Rui J, Ding X and Yang X: Exploring the multicomponent synergy mechanism of Banxia Xiexin Decoction on irritable bowel syndrome by a systems pharmacology strategy. J Ethnopharmacol 233: 158-168, 2019.
32. Li X, Xu X, Wang J, Yu H, Wang X, Yang H, Xu H, Tang S, Li Y, Yang L, *et al*: A system-level investigation into the mechanisms of Chinese traditional medicine: Compound danshen formula for cardiovascular disease treatment. PLoS One 7: e43918, 2012.
33. Zhang P, Zhang D, Zhou W, Wang L, Wang B, Zhang T and Li S: Network pharmacology: Towards the artificial intelligence-based precision traditional Chinese medicine. Brief Bioinform 25: bbad518, 2023.
34. Hu X, Li J, Fu M, Zhao X and Wang W: The JAK/STAT signaling pathway: From bench to clinic. Signal Transduct Target Ther 6: 402, 2021.
35. Fruman DA and Rommel C: PI3K and cancer: Lessons, challenges and opportunities. Nat Rev Drug Discov 13: 140-156, 2014.
36. Ma J, Matkar S, He X and Hua X: FOXO family in regulating cancer and metabolism. Semin Cancer Biol 50: 32-41, 2018.
37. Bosch-Barrera J and Menendez JA: Silibinin and STAT3: A natural way of targeting transcription factors for cancer therapy. Cancer Treat Rev 41: 540-546, 2015.
38. Liakopoulou C, Kazazis C and Vallianou NG: Silimarin and cancer. Anticancer Agents Med Chem 18: 1970-1974, 2018.
39. Kim SH, Choo GS, Yoo ES, Woo JS, Lee JH, Han SH, Jung SH, Kim HJ and Jung JY: Silymarin inhibits proliferation of human breast cancer cells via regulation of the MAPK signaling pathway and induction of apoptosis. Oncol Lett 21: 492, 2021.
40. Yu L, Li T, Zhang H, Ma Z and Wu S: Silymarin suppresses proliferation of human hepatocellular carcinoma cells under hypoxia through downregulation of the HIF-1α/VEGF pathway. Am J Transl Res 15: 4521-4532, 2023.
41. Borensztejn A, Boissoneau E, Fernandez G, Agnès F and Pret AM: JAK/STAT autocontrol of ligand-producing cell number through apoptosis. Development 140: 195-204, 2013.
42. Weber-Nordt RM, Mertelsmann R and Finke J: The JAK-STAT pathway: signal transduction involved in proliferation, differentiation and transformation. Leuk Lymphoma 28: 459-467, 1998.
43. Bharti AC, Shishodia S, Reuben JM, Weber D, Alexanian R, Raj-Vadhan S, Estrov Z, Talpaz M and Aggarwal BB: Nuclear factor-kappaB and STAT3 are constitutively active in CD138+ cells derived from multiple myeloma patients, and suppression of these transcription factors leads to apoptosis. Blood 103: 3175-3184, 2004.
44. Corvinus FM, Orth C, Moriggl R, Tsareva SA, Wagner S, Pfitzner EB, Baus D, Kaufmann R, Huber LA, Zatloukal K, *et al*: Persistent STAT3 activation in colon cancer is associated with enhanced cell proliferation and tumor growth. Neoplasia 7: 545-555, 2005.
45. Hodge DR, Hurt EM and Farrar WL: The role of IL-6 and STAT3 in inflammation and cancer. Eur J Cancer 41: 2502-2512, 2005.
46. Shi Z, Zhou Q, Gao S, Li W, Li X, Liu Z, Jin P and Jiang J: Silibinin inhibits endometrial carcinoma via blocking pathways of STAT3 activation and SREBP1-mediated lipid accumulation. Life Sci 217: 70-80, 2019.
47. Soleimani V, Delghandi PS, Moallem SA and Karimi G: Safety and toxicity of silymarin, the major constituent of milk thistle extract: An updated review. Phytother Res 33: 1627-1638, 2019.
48. Yao ZJ, Dong J, Che YJ, Zhu MF, Wen M, Wang NN, Wang S, Lu AP and Cao DS: TargetNet: A web service for predicting potential drug-target interaction profiling via multi-target SAR models. J Comput Aided Mol Des 30: 413-424, 2016.

49. Gfeller D, Grosdidier A, Wirth M, Daina A, Michielin O and Zoete V: SwissTargetPrediction: A web server for target prediction of bioactive small molecules. Nucleic Acids Res 42 (Web Server Issue): W32-W38, 2014.
50. Bosc N, Atkinson F, Felix E, Gaulton A, Hersey A and Leach AR: Large scale comparison of QSAR and conformal prediction methods and their applications in drug discovery. J Cheminform 11: 4, 2019.
51. Liu Z, Guo F, Wang Y, Li C, Zhang X, Li H, Diao L, Gu J, Wang W, Li D and He F: BATMAN-TCM: A bioinformatics analysis tool for molecular mechANism of traditional Chinese medicine. Sci Rep 6: 21146, 2016.
52. Szklarczyk D, Santos A, von Mering C, Jensen LJ, Bork P and Kuhn M: STITCH 5: Augmenting protein-chemical interaction networks with tissue and affinity data. Nucleic Acids Res 44 (D1): D380-D384, 2016.
53. Wishart DS, Feunang YD, Guo AC, Lo EJ, Marcu A, Grant JR, Sajed T, Johnson D, Li C, Sayeeda Z, *et al*: DrugBank 5.0: A major update to the DrugBank database for 2018. Nucleic Acids Res 46 (D1): D1074-D1082, 2018.
54. Wang Y, Zhang S, Li F, Zhou Y, Zhang Y, Wang Z, Zhang R, Zhu J, Ren Y, Tan Y, *et al*: Therapeutic target database 2020: Enriched resource for facilitating research and early development of targeted therapeutics. Nucleic Acids Res 48 (D1): D1031-D1041, 2020.
55. Gaulton A, Hersey A, Nowotka M, Bento AP, Chambers J, Mendez D, Mutowo P, Atkinson F, Bellis LJ, Cibrián-Uhalte E, *et al*: The ChEMBL database in 2017. Nucleic Acids Res 45 (D1): D945-D954, 2017.
56. Davis AP, Wiegers TC, Johnson RJ, Sciaky D, Wiegers J and Mattingly CJ: Comparative toxicogenomics database (CTD): Update 2023. Nucleic Acids Res 51 (D1): D1257-D1262, 2023.